Applied Surface Science 258 (2012) 3750–3756

Contents lists available at SciVerse ScienceDirect

Applied Surface Science

journal homepage: www.elsevier.com/locate/apsusc

Synthesis and conformational characterization of functional di-block copolymer brushes for microarray technology

Gabriele Di Carlo[a], Francesco Damin[a], Lidia Armelao[b], Chiara Maccato[c], Selim Unlu[d,e], Philipp S. Spuhler[e], Marcella Chiari[a,*]

[a] Institute of Chemistry of Molecular Recognition, National Research Council of Italy, Via M. Bianco 9, 20131 Milano, Italy
[b] ISTM-CNR and INSTM, Department of Chemistry, University of Padova, Via F. Marzolo 1, 35131 Padova, Italy
[c] Department of Chemistry and INSTM, University of Padova, Via F. Marzolo 1, 35131 Padova, Italy
[d] Department of Electrical and Computer Engineering, Boston University, St. Mary Street 8, Boston, MA 02215, United States
[e] Department of Biomedical Engineering, Boston University, St. Mary Street 8, Boston, MA 02215, United States

ARTICLE INFO

Article history:
Received 16 June 2011
Received in revised form
20 September 2011
Accepted 3 December 2011
Available online 13 December 2011

Keywords:
Surface initiated polymerization
Reversible addition–fragmentation chain transfer polymerization (RAFT)
Block copolymers
Polymer brushes
DNA microarray

ABSTRACT

Surface initiated polymerization (SIP) coupled with reversible addition-fragmentation chain transfer polymerization (RAFT) was used to functionalize microarray glass slides with block polymer brushes. N,N-dimethylacrylamide (DMA) and N-acryloyloxysuccinimide (NAS) (*graft*-poly[DMA-*b*-(DMA-*co*-NAS)]) brushes, with di-block architecture, were prepared from a novel RAFT chain transfer agent bearing a silanating moiety (RAFT silane) directly anchored onto the glass surfaces. Conformational characterization of the coatings was performed by Self Spectral Interference Fluorescence Microscopy (SSFM), an innovative technique that describes the location of a fluorescent DNA molecule relative to a surface with sub-nanometer accuracy. X-ray Photoelectron Spectroscopy (XPS) and Scanning Electron Microscopy (SEM) were used to characterize the coatings composition and morphology.

1. Introduction

Many of the methods used in genomics or proteomics are based on solid phase hybridization or complexation reactions between surface immobilized probes and free solution targets. Protein and DNA microarrays are examples of technologies for the simultaneous detection and quantification of a large number of biomolecules based on this principle. Chemical or biochemical reactions between free fluid components and immobilized probes require that an adequate number of molecules, with appropriate conformation, are immobilized on the surface. The most commonly used immobilization methods on glass surfaces involve the deposition of reactive silane films with terminal functional groups that react with biomolecules, either directly or through a subsequent modification. However, steric hindrance may significantly reduce the reaction between surface functional groups and probe molecules on these types of monodimensional coatings, leading to poor grafting density. A more advantageous method of immobilization implies the formation of a chemically reactive polymer film on the glass surface [1–5]. A polymeric coating is needed to control the local chemical environment so as to retain the native conformation of proteins [6]. In addition, polymer coatings provide a three dimensional binding scaffold, which leads to a substantial increase in the density of probes per unit area.

Homo- and block-copolymers brushes bearing chemical functionalities for the covalent attachment of biomolecules can be obtained by "grafting-onto" or "grafting-from" methods [7–13].

In this work, by using a "grafting from" approach we have functionalized glass substrates with brushes obtained by surface initiated (SI) controlled radical polymerization (CRP) [14]. CRP techniques, including nitroxide-mediated radical polymerization (NMP) [15], atom transfer radical polymerization (ATRP) [16] and reversible addition–fragmentation chain transfer polymerization (RAFT) [17], are excellent methods for the preparation of well-defined polymer structures such as block copolymers, star shape polymers, and interpenetrating polymer networks [18]. In particular, RAFT has recently emerged as a promising controlled radical polymerization technique due to its versatility and simplicity. A major advantage of RAFT polymerization over other processes for living/controlled free-radical polymerization is its compatibility with a wide range of monomers including functional monomers.

* Corresponding author. Tel.: +39 02 28500035.
E-mail address: marcella.chiari@icrm.cnr.it (M. Chiari).

0169-4332/$ – see front matter © 2011 Elsevier B.V. All rights reserved.
doi:10.1016/j.apsusc.2011.12.019

There is an increasing number of SI block brushes produced by CRP techniques but only few of them incorporate chemically reactive monomers in the external block [19]. In this work, a method to prepared a bioreactive coating made of N,N-dimethylacrylamide (DMA) and N-(acryloyloxy)succinimide (NAS) was devised and the "diblock" structure of the coating was confirmed by functional experiments, based on solid phase DNA hybridization, and by direct evaluation of the film conformation.

2. Experimental

2.1. Chemicals

N-hydroxysuccinimide (99%, NHS), acryloyl chloride (97%), triethylamine (≥99.5%, TEA), dichloromethane (≥99.5%; H_2O ≤0.005%), (3-aminopropyl)-trimethoxysilane (97%, APS), γ-mercaptopropyl trimethoxysilane (>95%, γMPS), 2-bromopropionylbromide (97%), phenylmagnesium bromide (1.0 M in THF), carbon disulfide (99.9%), tetrahydrofuran anhydrous (99.9%, inhibitor-free, THF), sodium sulfate (≥99%), S-(thiobenzoyl)thioglycolic acid (99%), 2-methyl-2-propanethiol (99%), hydrogen peroxide (30% in H_2O), ammonium hydroxide solution (28% in H_2O), octyl-trimethoxysilane (96%, nOS), sodium hydroxide (97%), N,N-dimethylacrylamide (99%, DMA), molecular sieves (4 Å, beads, 8–12 mesh), and microscope glass slides (75 mm × 25 mm) were purchased from Sigma–Aldrich. N,N-dimethylformamide (>99.8%, DMF), α,α′-azobisisobutyronitrile (≥98%, AIBN), aluminium oxide were purchased from Fluka. Diethyl ether (99.9%) was purchased from VWR. Toluene (>99.7%) was purchased from Riedel-de Haën. Davisil 663XW (500 Å pore size, 78–85 m^2/g surface area) was purchased from Supelco (Bellefonte, PA). The monomer N-(acryloyloxy)succinimide (NAS) [20] and the free chain transfer agent *tert*-butyl dithiobenzoate (tBDB) [21] were synthesized as previously reported.

2.2. Synthesis of 1-oxo-1-(3-(trimethoxysilyl)propylamino)propan-2-yl benzodithioate (RAFT silane, **2**) (Scheme 1)

At 0 °C a solution of 2-bromo propionyl bromide (2.83 mL, 0.027 mol) in dichloromethane (5 mL) was added dropwise to a stirred solution of (3-aminopropyl)-trimethoxysilane (APS; 4.86 mL, 0.027 mol) and triethylamine (TEA; 3.77 mL, 0.027 mol) in dichloromethane (30 mL). The solution was stirred at room temperature under nitrogen pressure for 2 h, then it was filtered and evaporated under vacuum. The crude product was purified by bulb-to-bulb distillation (175 °C, 1 mBar) to form the bromine derivative (**1**) as a colorless oil (7.6 g, 0.024 mol, 89% yield). ^{1}H NMR (300 MHz, $CDCl_3$) δ (ppm): 6.60 (1H, NH), 4.40 (q, 1H, −CHBr), 3.55 (s, 9H, OCH_3), 3.25 (m, 2H, $-CH_2N$), 1.85 (d, 3H, $-CH_3$), 1.65 (m, 2H, $-CH_2-$), 0.65 (m, 2H, $Si-CH_2-$).

In a second step, CS_2 (2.9 mL, 0.048 mol) was slowly added at 0 °C to a stirred solution of phenylmagnesium bromide (1 M in THF, 25.4 mL, 0.025 mol). The solution was stirred at room temperature under nitrogen pressure for 1.5 h and then cooled at 0 °C. A solution of **1** (7.6 g, 0.024 mol) in THF (10 mL) was added dropwise. The mixture was then allowed to react overnight at room temperature, and the solvent was evaporated under vacuum. The resulting residue was dissolved in CH_2Cl_2 (15 mL), washed with water and brine and dried with Na_2SO_4. The RAFT silane (**2**) was obtained as a red oil (6.6 g, 0.017 mol, 69% yield) and used without further purification. ^{1}H NMR (300 MHz, $CDCl_3$) δ (ppm): 7.15–8.10 (m, 5H, phenyl), 6.60 (1H, NH), 4.75 (q, 1H, −CHBr), 3.55 (s, 9H, OCH_3), 3.25 (m, 2H, $-CH_2N$), 1.85 (d, 3H, $-CH_3$), 1.65 (m, 2H, $-CH_2-$), 0.65 (m, 2H, $Si-CH_2-$).

2.3. Silica surfaces functionalization

Microscope glass slides pretreatment. Glass slides were cleaned and activated in a Harrick Plasma Cleaner for 15 min at high radio frequency level by oxygen-plasma.

RAFT silane functionalization. Glass slides were dipped in a solution of RAFT silane and octyltrimethoxysilane (nOS) in toluene for 4 h at room temperature under nitrogen atmosphere. The ratios between RAFT silane and nOS are reported in Table 1. After the reaction was completed, the slides were washed with fresh toluene and THF and then dried in a vacuum oven at room temperature for 30 min.

2.4. Synthesis of graft-poly(DMA) via RAFT polymerization (Scheme 2)

A 100 mL solution of DMA (45.95 mL, 0.446 mol, filtered on aluminium oxide to remove inhibitors), tBDB (0.262 g, 0.125×10^{-2} mol) and AIBN (0.041 g, 0.025×10^{-2} mol) in dry toluene (dried on molecular sieves) was degassed under argon at 0 °C for 1 h. Silanized slides (see Table 1) were immersed overnight in the monomer solution brought to 80 °C under nitrogen atmosphere, then Soxhlet extracted with THF for 12 h. The slides were finally dried under N_2 flow.

2.5. Synthesis of graft-poly[DMA-b-(DMA-co-NAS)] via free radical polymerization (Scheme 2)

The extension of poly(DMA) to form the active block of poly[DMA-*b*-(DMA-*co*-NAS)] as reported in Scheme 2, was carried out by polymerizing a mixture DMA (9.27 mL, 0.09 mol, filtered on aluminium oxide to remove inhibitors), NAS (1.69 g, 0.01 mol) and AIBN (9.2 mg, 0.056×10^{-3} mol) in 100 mL of DMF (dried on molecular sieves), degassed under argon at 0 °C for 1 h. Slides coated with the first block of poly(DMA) were immersed overnight in the reaction mixture at 80 °C under nitrogen atmosphere, Soxhlet extracted with THF for 12 h and dried in a vacuum oven at room temperature for 2 h. To the same solution, slides derivatized with RAFT silane/nOS 1:1 were also added to produce *graft*-Poly(DMA-*co*-NAS) coated slides in which the functional copolymer was directly attached to the surface without the intermediate layer of poly(DMA) (monoblock coating).

2.6. DNA–DNA hybridization test

A SciFlexArray spotter (Scienion, Berlin, Germany) was used to pattern a subarray of a 23-mer oligonucleotide of sequence 5′-NH_2-$(CH_2)_6$-GCC CAC CTA TAA GGT AAA AGT GA). The oligonucleotide was dissolved at 10 μM concentration in sodium phosphate buffer (150 mM, 0.01% Triton, pH 8.5). The volume of spotted drops was 400 pL. In each printed array (100 replicated spots), the diameter of the spots was ∼100 μm. After probe deposition, the slides were placed in an uncovered storage box placed in a sealed chamber, saturated with NaCl, and incubated at room temperature overnight.

Unreacted sites on the slides were blocked with a 50 mM solution of ethanolamine in 0.1 M Tris–HCl at pH 9 for 15–20 min at 50 °C, rinsed with water and then washed in 4× saline-sodium citrate (SSC) buffer/0.1% w/v sodium dodecilsulfate (SDS) for 15–20 min at 50 °C. An oligonucleotide target (23-mer Cy3-oligonucleotide labelled at the 5′ terminus) complementary to the sequence of the immobilized probe was dissolved in the hybridization buffer (5× SSC/0.1% w/v SDS/0.02% w/v bovine serum albumine-BSA) and immediately applied to the microrrays. After hybridization (2 h, 65 °C), the slides were first washed in 2× SSC/0.1% SDS buffer (10 min, 65 °C) and rinsed with 0.2 × SSC (1 min), followed by a rinse with 0.1× SSC (1 min). Scanning for

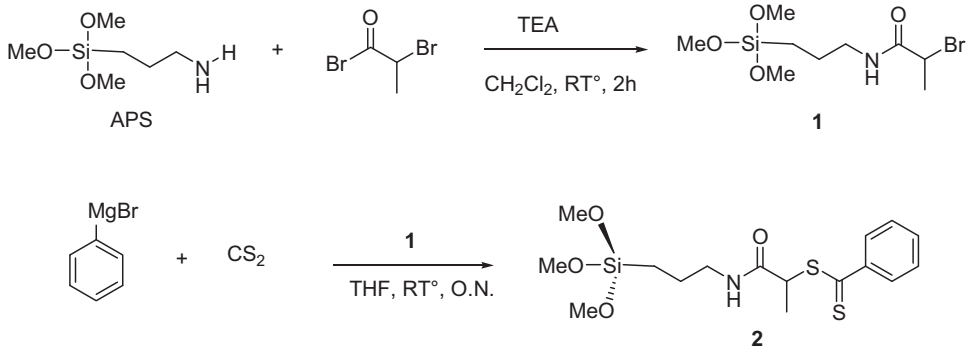

Scheme 1. Synthesis procedure of 1-oxo-1-(3-(trimethoxysilyl)propylamino)propan-2-yl benzodithioate (RAFT silane, **2**).

Table 1
Different concentrations of RAFT silane and nOS in the silanization solution.

	A	B	C	D	E
RAFT silane[a] (mol × L^{-1})	2.5×10^{-3}	2×10^{-3}	1.25×10^{-3}	0.5×10^{-3}	–
nOS[b] (mol × L^{-1})	–	0.5×10^{-3}	1.25×10^{-3}	2×10^{-3}	2.5×10^{-3}

[a] RAFT silane: 1-oxo-1-(3-(trimethoxysilyl)propylamino)propan-2-yl benzodithioate.
[b] nOS: *n*-octyltrimethoxyilane.

fluorescence evaluation was performed with a Scan Array Express scanner from Packard Bioscience (Boston, MA).

2.7. Self spectral interference fluorescence microscopy

The principle of operation of SSFM, the experimental set-up for data acquisition, and the processing of the spectra for nanometer accuracy in axial localization were reported previously [22]. Briefly, the system consists of a continuous wave laser for excitation, a microscope, and a spectrometer. In this study, the laser beam (He–Ne at 633 nm) is coupled to the microscope objective (0.12 numerical aperture) through the side port of an upright microscope and focused onto the sample. The fluorescence signal is collected with the same objective, coupled to a spectrometer with 1800 groves/mm grating (spectral resolution of 1 cm^{-1} at 700 nm) for spectral acquisition, and the signal is recorded using a thermoelectrically cooled CCD. The spectra are then fitted with a custom-built MATLAB application that returns the average height of the biolayer and the average height of the fluorophores from the silicon oxide/silicon interface. The results obtained with SSFM are immune to factors that can affect the total signal such as the local fluorophore density or photobleaching, since the spectral oscillations, rather than the total emission intensity, are used for determining the position of the emitters.

2.8. X-ray photoelectron spectroscopy

XPS analyses were performed with a Perkin Elmer Φ 5600-ci spectrometer using non mono-chromatized (15 kV, 400 W) Al-Kα radiation (1486.6 eV). The samples were mounted on a steel sample holder and introduced directly, by a fast-entry lock system, into the XPS analytical chamber. The sample analysis area was 800 μm in diameter and the working pressure was $<5 \times 10^{-8}$ Pa. The spectrometer was calibrated assuming the binding energy (BE) of the Au4f$_{7/2}$ line at 83.9 eV with respect to Fermi level. The standard deviation for the BE values was ± 0.2 eV. Charging

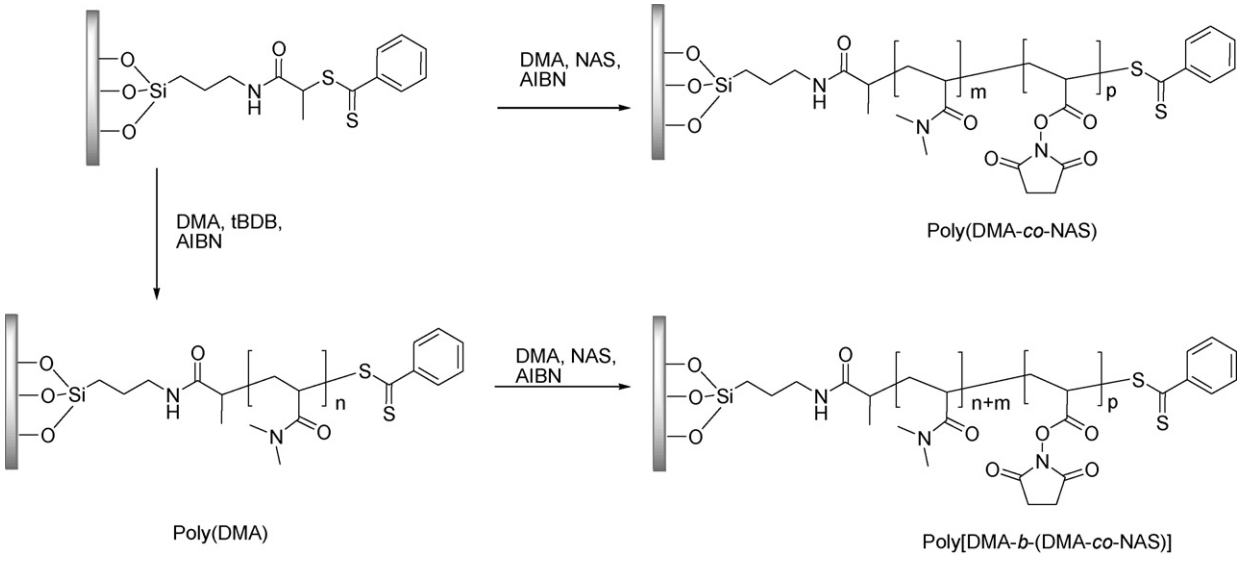

Scheme 2. Schematic synthesis of the RAFT mediated brush polymers: mono-block and di-block architectures.

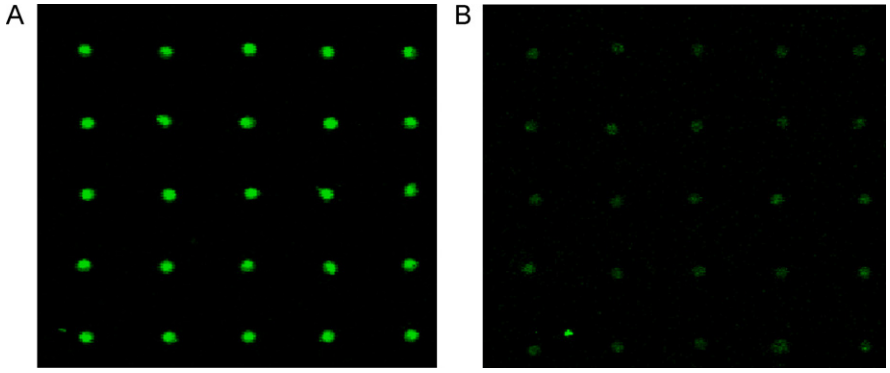

Fig. 1. Fluorescence of oligonucelotide spots in an oligo/ologo hybridization assay: (A) *Graft*-poly[DMA-b-(DMA-co-NAS)] brush coating, synthesized onto a glass slide functionalized with RAFT silane/nOS in 1:1 ratio. (B) negative control experiment. No functional polymer was formed on a slide modified only with nOS when subjected to the same treatments as slide shown in A.

effects were corrected by assigning to the C 1s peak associated with adventitious hydrocarbons a value of 284.8 eV [23]. Survey scans were run in the 0–1300 eV range, while detailed scans were recorded for the C 1s, N 1s, O 1s, Si 2p and S 2p regions. No further element was detected. The analyses involved Shirley-type background subtraction and spectral deconvolution, which was carried out by non-linear least-squares curve fitting, adopting a Gaussian–Lorentzian sum function.

2.9. GPC-MALLS analysis

The polymers obtained during the production of the poly(DMA) (macro-CTA) and poly(DMA-co-NAS) blocks were recovered from polymerization solutions by precipitation in ethyl ether. They were fractionated using aqueous Gel Permeation Chromatography (GPC) and then characterized using a on-line Multi-Angle Laser Light Scattering (MALLS) detector and a refractive index detector.

The GPC scheme consists of four Shodex aqueous GPC columns in series, OHpak SB-G (guard column), OHpak SB-806M HQ, OHpak SB-804 HQ, and OHpak SB-802.5 HQ, maintained at 25 °C using an Agilent 1200 thermostated column compartment. The MALLS instrument is a DAWN HELEOS II (Wyatt Technology), which detects scattered light at 18 angles measuring the radius (R_g) as well as the absolute molecular weight (M_w and M_n) of the polymer in solution. The MALLS instrument was in-line with an Optilab rEX (Wyatt Technology) refractive index detector. Samples were diluted using the GPC mobile phase (GPC buffer: 100 mM NaCl, 50 mM NaH_2PO_4, 200 ppm NaN_3), both to a concentration of 2 mg/mL. The flow rate through the GPC-MALLS system was kept constant at 0.3 mL/min value. The samples were analyzed three times through the GPC-MALLS to test for reproducibility. Each run injected 100 μL of sample to be analyzed. The averaged results and the relative standard deviations between runs are summarized in Table 2.

3. Results and discussion

A diblock copolymer brush coating was synthesized via surface initiated controlled radical polymerization (CRP) using a novel iniferter immobilized on a glass slide surface whose chemical structure is reported in Scheme 1. The diblock polymer enables control of the location of chemical reactive moieties leading to immobilization of probes that, being spaced from the solid surface, are more prone to interact with their solution targets. In a dense monoblock architecture, some of the probes being partially buried in the polymeric structure might be unavailable for binding large DNA fragments [24].

A simple DNA hybridization experiment was performed to prove the confinement of active esters on the external block. An amino modified oligonucleotide was spotted on the surface and hybridized with a fluorescently labelled complementary oligonucleotide. In Fig. 1A, a typical fluorescence image of a DNA microarray obtained with the diblock coating is shown. Only slides modified by the RAFT silane gave rise to formation of a coating able to bind oligonucleotides. Due to the confinement of the chemically reactive monomer on the external block, the experiment of Fig. 1 proves the formation of the second block. In Fig. 2 the intensity of fluorescence obtained in the hybridization of complementary oligonucleotides on the various slides (A–E) shown in Table 1 is reported. Slides either coated only by a poly(DMA) block or modified by 100% nOS were unable to bind oligonucleotides as demonstrated by the complete lack of fluorescent after hybridization (Fig. 1B). Modifying the substrate from which the brush is grown with a mixture of initiator-functionalized compound and a "dummy" compound, that is not able to initiate the polymerization reaction, is a common way to control brush density. As clearly shown in Fig. 2, reduction of RAFT initiator probably resulting in brush density reduction does not affect hybridization efficiency which is similar on the various substrates, from A to D. However, fluorescence intensity on slides coated by the di-block copolymer increases on slides where the density of RAFT compound is reduced by the use of a dummy compound. The binding capacity of the external polymer segment reaches a maximum value on polymer coating grown on glass

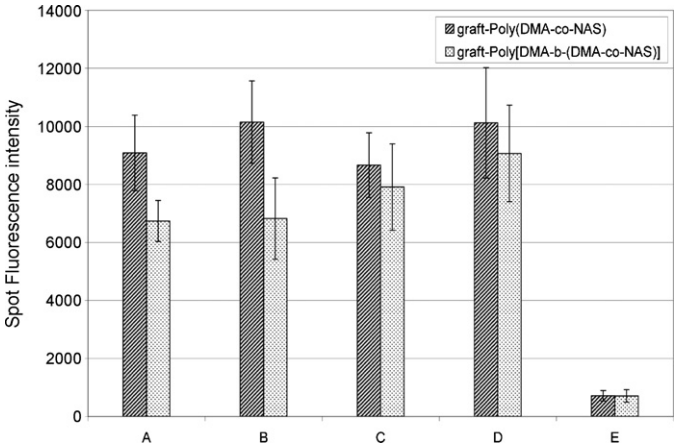

Fig. 2. Fluorescence of oligonucelotide spots in an hybridization test: average fluorescence of 100 replicated spots on poly(DMA-co-NAS) (first active block) and on poly[DMA-b-(DMA-co-NAS)] (second active block) synthesized onto different ratio of RAFT silane/nOS functionalized glass slides (Table 1).

Table 2
Results from GPC-MALLS analysis of the polymers recovered from polymerization solution.

Polymer sample	M_n[a] (g/mol)	M_w[b] (g/mol)	PDI[c] (M_w/M_n)	R_g[d] (nm)
poly(DMA)	23,080	35,620	1.544	6.40
RSD (%)[e]	0.7	2.0	2.7	11.8
poly(DMA-co-NAS)	14,180	45,360	3.200	10.00
RSD (%)[e]	4.8	2.5	2.2	1.0

[a] Number-average molecular weight.
[b] Weight-average molecular weight.
[c] Polydispersity index.
[d] Radius of gyration (root mean squared radius).
[e] Relative standard deviation (RSD).

surfaces modified with a 0.25:1 RAFT silane/nOs ratio. This effect might be due to a better control on the migration of graft radicals on contiguous chains, an event that would reduce the "livingness" of the first polymeric block [16]. The intensity of fluorescence measured on the di-block copolymer is not higher than that found on the mono-block coating because the density of chains containing NHS is significantly lower in the second block. This is somehow expected as only some of the chains maintain their "leaving character" and are able to give rise to formation of the second block. The proximity of probes to a solid surface, especially for protein probes, generally leads to reduced specificity of target binding and a loss of probe functionality. The surface proximity can also result in interactions between the target and the surface, which may further hinder specific probe–target binding. A related effect is the orientation immobilized probes; for randomly oriented probe proteins a large portion of the active sites may be inaccessible to targets in solution. This is especially likely for probe proteins that are randomly oriented on a solid, as the active binding site will be obstructed by the solid surface for a majority of the probes [25]. However, for probes immobilized on a polymeric scaffold, the effects of orientation are mitigated because binding sites can remain accessible if the polymer permits diffusion of the target protein to the probe binding site.

The aim of our work was to demonstrate by self interference fluorescence microscopy (SSFM) the confinement of binding sites on the external part of the polymer brush and to accurately measure the distance of a probe relative to the surface.

3.1. Conformational characterization

In the di-block coating proposed, the localization of probes few tenths of nanometers away from the surface was proven by self interference fluorescence microscopy (SSFM), an innovative technique that allows quantification of the vertical distance of a fluorophore from a surface with sub-nanometer resolution [26]. In SSFM, fluorescent labels are attached to one end of DNA tethered to a glass surface. Light is bounced off the top surface of the DNA layer, but it also travels through and bounces off a reflective bottom surface. The interaction of the two wavelengths – one reflected from the fluorescent label, the other from the bottom layer – produces oscillations in the spectrum of the returning light. The pattern of oscillations, or interference spectrum, describes the location and shape of the DNA molecule with sub-nanometer accuracy. Fluorescent single stranded and double stranded 23 mer oligonucleotides modified with amine groups on the 5′ (surface proximal) end and cyanine 5 on the 3′ end, were immobilized on a silicon substrate coated with a 17 μm silicon oxide layer. The SiO_2 chips were activated for the covalent binding either with a mono block brush coating of copoly(DMA-NAS) or with a di-block brush coating of poly[DMA-*b*-(DMA-co-NAS)]. The average fluorophore height was measured by SSFM under dry (dried under argon flow and left under vacuum overnight) and wet conditions (2× SSC and 0.1% SDS) for each spot in the array of ssDNA and dsDNA. Fig. 3 shows a histogram of the average fluorophore height change from dry to wet conditions. The height differences at each spot in the two samples are shown. The difference in the detected average fluorophore height on the dry and hydrated polymeric film indicates an increase in the length of polymer chain due to the swelling. We observe a 3–4 nm differences in the height changes between ssDNA and dsDNA spotted on the mono and di-block brush coated chips. This is accounted for by the different conformations between ssDNA and dsDNA. Whereas the ssDNA probes are highly flexible and assume a random orientation around the functional NAS groups, the double stranded DNA probes are stiff and assume an orientation of 33° to the surface. As the root mean square end-to-end length of the short dsDNA probes is about 7.8 nm, the expected height difference between fluorophore tags on ssDNA and dsDNA probes is approximated by

$$\Delta h = \sin(\theta)\sqrt{< R^2 >}$$

where θ is the mean probe orientation with respect to the surface and $\sqrt{< R^2 >}$ is the root mean square end-to-end probe length. This gives a mean height change of 3.9 nm, due to the conformational difference between the ssDNA and dsDNA.

Previous studies on the penetration depth of ssDNA and dsDNA to similar polymer brush coatings found that the non-specific DNA binding is minimal and the average penetration is due mainly to the spatial distribution NAS blocks that bind to the amine groups on the DNA [27]. The increased swelling ability of the di-block poly[DMA-*b*-(DMA-coNAS)] brush coating (almost three times that of the mono block) is a result of the low density of chains belonging to the second block versus the chains of the first block. If the chains are in a highly dense brush conformation, no room is available for them to sit on the surface when they are dry, thus leading to a less significant extension hydrated conditions. On the contrary, the chains of the second block could be less compact, approaching a mushroom conformation from which a full extension is favored. SSFM demonstrates the effectiveness of RAFT modified surfaces to form di-block polymeric films with functional groups confined in the external polymer segment.

Molecular weight and polydispersity of the polymers recovered from the feed after polymerization of the first and of the second block were assessed by gel permeation chromatography (GPC). Although not generally accepted, some articles suggest that polydispersity (PDI) and molecular weight (M_w) [28–30] of surface polymers can be inferred from those of solution polymers. From the GPC-MALLS analysis (Table 2) on poly(DMA) and poly(DMA-*co*-NAS), it appears that the thickness of the coating is higher than the sum of the gyration radius of the polymer segments that form the two blocks. This is typical of "brush type" coatings in which the high chain density forces the polymer to assume an extended conformation. In the synthesis of the second block, a non controlled radical polymerization was adopted to form a "mushroom type" coating. This architecture is more suitable to promote highly efficient and specific capture of proteins and DNA in solid phase assays. Finally, SEM analysis by Zeiss SUPRA 40VP (data not shown) revealed that

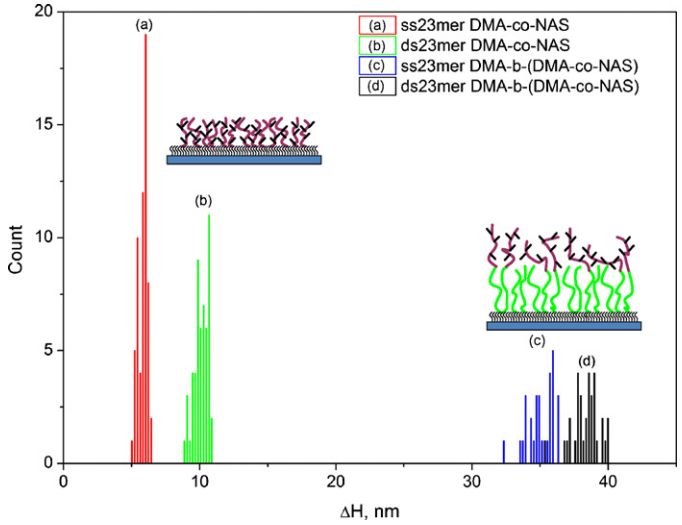

Fig. 3. Average fluorophore height measured by SSFM under dry (dried under argon flow and left under vacuum overnight) and wet conditions (2× SSC and 0.1% SDS) for each spot in the array of ssDNA and dsDNA.

the coatings are homogeneous and crack-free, confirming thus the effectiveness of the adopted grafting procedure.

3.2. Chemical characterization

The chemical composition of the polymer films on the surface was assessed by X-ray photoelectron spectroscopy. On each chip a survey scan was collected to identify the chemical species present on the sample surface. Detailed scans were subsequently recorded for the XPS regions of interest. Survey scan from a freshly cleaned and activated silica slide exhibits peaks from Si 2p and Si 2s lines as well as the presence of C 1s and O 1s signals. While carbon is associated to adventitious surface contamination (C 1s BE = 284.8 eV), oxygen and silicon peaks are unambiguously related to the silica (O 1s BE = 532.9 eV, Si 2p BE = 103.8 eV) [21]. The amount of adventitious carbon contamination is about 7% at. of the total elemental composition (C/Si ∼ 0.3). In order to estimate the degree of grafting of CTA silane and polymer chains on the silica surface, a detailed XPS analysis of C 1s, O 1s, Si 2p, S 2p and N 1s peak shape and position for the different samples was performed.

Surface modified by CTASil: An intense C 1s peak at BE of 284.8 eV with a lower intensity shoulder on the high energy side is found on the sample surface. Peak fitting of the C 1s line reveals three components (Fig. 4) centred at 284.8 eV (C_I), 286.2 eV (C_{II}) and 287.8 eV (C_{III}), whose relative amount is 75%, 16% and 9%, respectively. The lower binding energy component is the fingerprint of hydrocarbon chains, whereas the two higher binding energy components can be respectively associated to single C–N, C–O and C–S bonds (C_{II}), and to carboxylic and/or thiocarboxylic moieties (C_{III}), respectively [23,31].

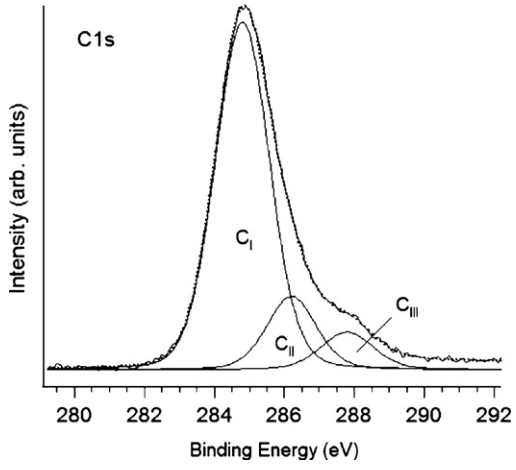

Fig. 4. C 1s region and fitting components for the blank sample.

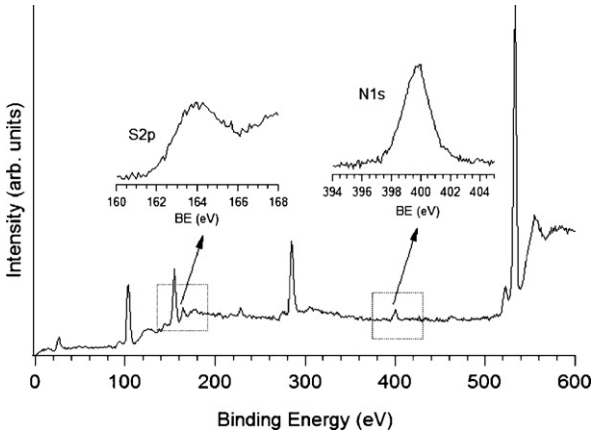

Fig. 5. Survey spectrum, detailed N 1s and S 2p regions for the RAFT silane coated sample.

Concerning the N 1s line, it consists in a single component peaked at 399.8 eV, typical of aminic nitrogen atoms [23]. As for sulphur, the S 2p region is peaked at 163.7 eV, which is typical for C–S bonds, whereas the presence of oxidized sulphur species can be ruled out [31] (Fig. 5). Quantitative analysis from peak area integration reveals a ∼ 1S:4N atomic ratio, that is sensibly lower than the expected nominal value, whereas the C:Si atomic ratio is *ca.* 1.

Surface modified by graft-Poly(DMA): In the survey spectrum, besides C 1s, O 1s, N 1s, silicon and sulphur-related lines, no further element is detected. Detailed analysis of C 1s peak reveals an increased intensity of the high-energy side shoulder (Fig. 6) corresponding to a larger content of C–N, C–O and C–S bonds, and carboxylic and/or thiocarboxylic moieties in the grafted layer. Indeed, the C1s line is fitted to three components in agreement with the results found in the previous case. The same considerations also apply to N 1s and S 2p regions, whose peak profile and position are consistent with the presence of aminic groups and C–S bonds. Quantitative analysis indicates that the nitrogen content is

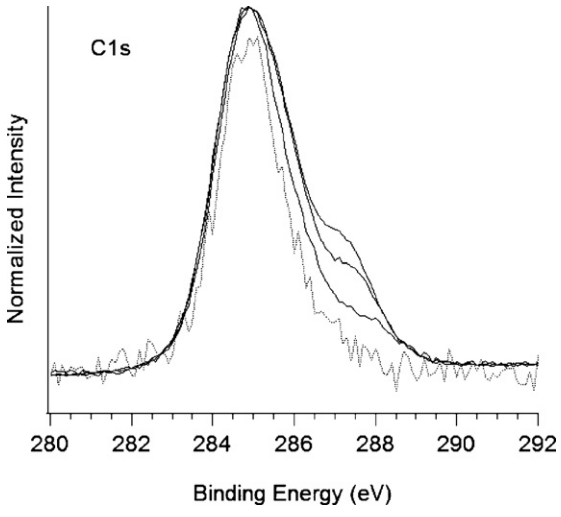

Fig. 6. C 1s profile (from bottom to top) for uncoated oxide, RAFT silane/nOS, *Graft* poly(DMA) and *Graft-Poly[DMA-b-(DMA-co-NAS)]* samples.

consistently increased, with a N:S atomic ratio on the order of 40, and that the C:Si ratio is *ca.* 6.

Surface modified with Graft-poly[DMA-b-(DMA-co-NAS)]: The XPS analysis results are qualitatively in agreement with the previously discussed cases. Accordingly, the C 1s line shows a further increase on the high energy shoulder, as reported in Fig. 6. Again, the spectral features of N 1s and S 2p lines resemble those of the other samples. The further increase of the C:Si atomic ratio to *ca.* 20, indicates the presence of a stably grafted layer on the pristine silicon surface, whose thickness is gradually increasing.

4. Conclusions

Surface initiated polymerization was coupled to reversible addition–fragmentation chain transfer (RAFT) process to produce a well-defined polymeric architecture on glass slides to be used in microarray technology. An effective and robust approach for the direct functionalization of glass surface with a novel RAFT agent was developed. The presence of an iniferter on the surface led to formation of bioreactive polymer coatings of well defined architecture. It was also demonstrated the polymeric film is composed by two layers, and that NAS functionalities that are present only in the external block allow to bind DNA probes at a distance of about 30 nm from the surface.

Mono- and di-block brushes were characterized by chemical and functional tests. The fluorescence intensities obtained by DNA–DNA hybridization tests on di-block polymeric coatings confirmed the ability of the RAFT mediated surfaces to promote the formation of living polymer chains. X-ray photoelectron spectroscopy confirmed the presence of sulphur atoms in the first polymer block which is an indication of the living character of grafted chains. SSFM provide a direct estimate of the thickness of the coating and prove the formation of a di-block architecture.

Acknowledgments

The authors thank Fondazione Cariplo, project Spintronc Biosensor for Medicine and FIRB Projects RBAP114AMK “RINAME” and RBPR05JH2P “Rete ItalNanoNet”.

References

[1] J.-S. Yang, T.M. Swager, J. Am. Chem. Soc. 120 (1998) 11864.
[2] D.M. Bubb, R.A. McGill, J.S. Horwitz, J.M. Fitz-Gerald, E.J. Houser, P.W. Wu, B.R. Ringeisen, A. Piqué, D.B. Chrisey, J. Appl. Phys. 89 (2001) 5739.
[3] J. Kim, D.T. McQuade, S.K. McHugh, T.M. Swager, Angew. Chem., Int. Ed. 39 (2000) 3868.
[4] Y. Liu, M. Zhao, D.E. Bergbreiter, R.M. Crooks, J. Am. Chem. Soc. 119 (1997) 8720.
[5] Y. Ito, Y.S. Park, Y. Imanishi, J. Am. Chem. Soc. 119 (1997) 2739.
[6] M. Cretich, G. Pirri, F. Damin, I. Solinas, M. Chiari, Anal. Biochem. 332 (2004) 67.
[7] P. Mansky, Y. Liu, E. Huang, T.P. Russell, C.J. Hawker, Science 275 (1997) 1458.
[8] Y. Geng, D.E. Discher, J. Justynska, H. Schlaad, Angew. Chem. Int. Ed. 45 (2006) 7578.
[9] D. Joester, B. Klein, E. Geiger, L. Addadi, J. Am. Chem. Soc. 128 (2006) 1119.
[10] W.S. Choi, J.H. Park, H.Y. Koo, J.Y. Kim, B.K. Cho, D.Y. Kim, Angew. Chem. Int. Ed. 44 (2005) 1096.
[11] M. Ulbricht, H. Yang, Chem. Mater. 17 (2005) 2622.
[12] B. Parrish, R.B. Breitenkamp, T. Emrick, J. Am. Chem. Soc. 127 (2005) 7404.
[13] K. Buga, A. Majkowska, R. Pokrop, M. Zagorska, D. Djurado, A. Pron, et al., Chem. Mater. 17 (2005) 5754.
[14] H.P. Brack, C. Padeste, M. Slaski, S. Alkan, H.H. Solak, J. Am. Chem. Soc. 126 (2004) 1004.
[15] M. Georges, R. Veregin, P. Kazmaier, G. Hamer, Macromolecules 26 (11) (1993) 2987–2988.
[16] K. Matyjaszewski, J. Xia, Chem. Rev. 101 (2001) 2921.
[17] J. Chiefari, Y.K. Chong, F. Ercole, J. Krstina, J. Jeffery, T. Le, R. Mayadunne, G. Meijs, C. Moad, G. Moad, E. Rizzardo, S.H. Thang, Macromolecules 31 (1998) 5559–5562.
[18] W.A. Braunecker, K. Matyjaszewski, Prog. Polym. Sci. 32 (2007) 93–146.
[19] G. Pirri, M. Chiari, F. Damin, A. Meo, Anal. Chem. 78 (2006) 3118–3124.
[20] M. Mammen, G. Dahmann, G.M. Whitesides, J. Med. Chem. 38 (1995) 4179–4190.
[21] A. Favier, M.-T. Charreyre, P. Chaumont, C. Pichot, Macromolecules 35 (2002) 8271–8280.
[22] A.K. Swan, L. Moiseev, C.R. Cantor, B.J. Davis, S.B. Ippolito, W.C. Karl, B.B. Goldberg, M.S. Ünlü, IEEE JSTQE 9 (2003) 294.
[23] J.F. Moulder, W.F. Stikle, P.E. Sobol, K.D. Bomben, Handbook of X-ray Photoelectron Spectroscopy, Perkin Elmer Corp., 1992.
[24] A. Haperin, A. Buhot, Langmuir 22 (2006) 11290–11304.
[25] T.W. Cha, A. Guo, X.Y. Zhu, Enzymatic activity on a chip: the critical role of protein orientation, Proteomics 5 (2005) 416–419.
[26] L. Moiseev, M.S. Ünlü, A.K. Swan, B.B. Goldberg, C.R. Cantor, PNAS 103 (2006) 2623.
[27] A. Yalcin, F. Damin, E. Ozkumur, G. Di Carlo, B.B. Goldberg, M. Chiari, M.S. Ünlü, Anal. Chem. 81 (2009) 625.
[28] Y. Tsujii, M. Ejaz, K. Sato, A. Goto, T. Fukuda, Macromolecules 34 (2001) 8872–8878.
[29] C. Li, B.C. Benicewicz, Macromolecules 38 (2005) 5929–5936.
[30] C. Li, J. Han, C.Y. Ryu, B.C. Benicewicz, Macromolecules 39 (2006) 3175.
[31] D. Briggs, M.P. Seah, Practical Surface Analysis, vol. 1, J. Wiley, Chichester, 1990.